Vortex Burst as a Source of Turbulence

Yannis Cuypers,[1] Agnès Maurel,[2] and Philippe Petitjeans[1]
[1]*Laboratoire de Physique et de Mécanique des Milieux Hétérogènes, UMR 7636, Ecole Supérieure de Physique et de Chimie Industrielles, 10 rue Vauquelin, 75005 Paris, France*
[2]*Laboratoire Ondes et Acoustique, UMR 7587, Ecole Supérieure de Physique et de Chimie Industrielles, 10 rue Vauquelin, 75005 Paris, France*
(Received 15 May 2003; published 3 November 2003)

An important issue in turbulence theory is to understand what kinds of elementary flow structures are responsible for the part of the turbulent energy spectrum described by Kolmogorov's celebrated $k^{-5/3}$ law. A model for such structure has been proposed by Lundgren [Phys. Fluids **25**, 2193–2203 (1982)] in the form of a vortex with spiral structure subjected to an axially straining field. We report experimental results of a vortex burst in a laminar-flow environment showing that this structure is responsible for a $k^{-5/3}$ part in the energy spectrum. If there are many experimental evidences of the existence of vortices with spiral structures in turbulent flows, it is the first time that such an elementary structure is experimentally shown to be responsible for the turbulent energy cascade.

DOI: 10.1103/PhysRevLett.91.194502 PACS numbers: 47.27.Ak, 47.27.Cn, 47.32.Cc

In 1982, Lundgren reported a model of a vortex, whose spatiotemporal characteristics provide a mechanism for an energy cascade from large to small spatial scales giving the Kolmogorov five-thirds spectrum characteristic of turbulent flows, provided that the usual spatial averaging is done over the lifetime of the vortex [1]. This model has received a growing interest in the last ten years, when it has begun to be understood that statistical laws in turbulence, including fully developed turbulence, are controlled by discrete structures. One problem is to give a physical representation of how a cascade can build up in a space containing these structures [2–4]. It is also of interest to understand the coexistence of coherent structures and the surrounding turbulence [5,6]. In the present Letter, we investigate the behavior of a single vortex whose environment makes it break periodically into turbulent burst. Contrary to classical experiments focusing on coherent structures in turbulence, no surrounding turbulent flow exists, so that the observed turbulence results only from the vortex burst. We find that the energy spectrum does follow a five-thirds law when averaged over the lifetime of the vortex burst and it is shown that this behavior results from a time evolution of the spectra, in agreement with Lundgren's theory. However, it is also shown that the instantaneous spectra experience a transition from a near k^{-1} behavior to a k^{-2} behavior, contrary to results obtained from numerical calculations performed on a Lundgren's single spiral vortex [7].

The water channel is represented in Fig. 1. Its section is 7 cm × 12 cm and the typical longitudinal velocity is a few cm s^{-1}. Details on the experimental apparatus can be found in [8]. A small step added to a laminar boundary layer profile in the bottom wall produces the initial vorticity that is strongly enhanced by the stretching produced by sucking the flow through slots on each lateral wall (slot diameter is 0.6 cm). A stretched vortex is produced, whose axis is attached at both extremities to the suction slots. At fixed value of the suction flowrate Q_2, varying the downstream flowrate Q_1 makes two regimes occur. Low values of Q_1 correspond to a stable, nearly stationary vortex. Above some critical value of Q_1(not discussed here), the vortex follows a periodic cycle : in the first stage of the cycle, it remains coherent while it is elongated under the influence of the flow, and in the second stage, it explodes in a turbulent burst; thereafter another vortex is generated and so on (visualizations of the two stages of the cycle using dye injection are shown in Fig. 2). In previous studies, the vortex has been characterized in terms of a coherent structure in both stable and unstable regimes [8–10].

Benefiting from previous measurements [9], we report in Table I the characteristics of the vortex when it breaks (in the present experiments, $Q_1 = 12.5\,\mathrm{l\,min^{-1}}$ and $Q_2 = 7.5\,\mathrm{l\,min^{-1}}$). Since measurements of the axial velocity $u_z(z)$ is not possible in the periodic regime, only a coarse estimation of the stretching $a \equiv \partial_z u_z$ is given, corresponding to measurements performed in the stable regime [10].

In order to better quantify the burst, local measurements of the velocity have been taken using a hot-film probe, located at a distance d from the z axis, as indicated in Fig. 1. The probe is set parallel to the axis of the

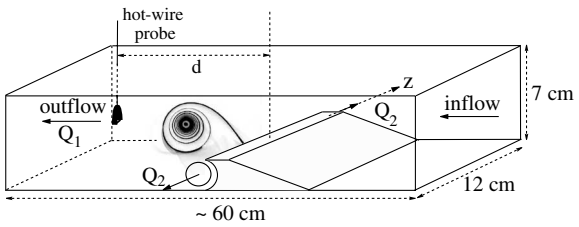

FIG. 1. Experimental setup.

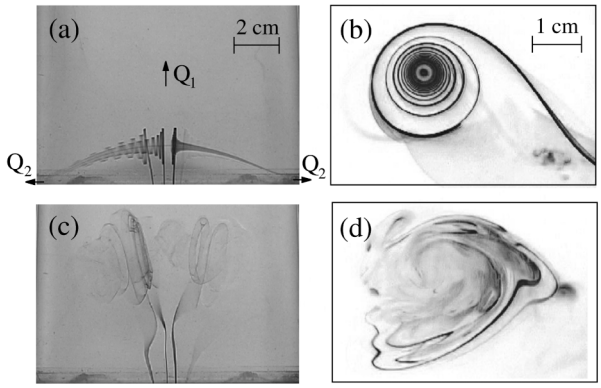

FIG. 2. Dye visualization of the vortex (top view on left and side view on right) for $Q > Q_c$: first (a),(b) and second (c),(d) stages of the cycle.

stretching so that it measures $U = \sqrt{u_r^2 + u_\theta^2}$. A typical time recording is shown on Fig. 3(a). It can be seen that a typical cycle is formed of two parts. In the first part, the velocity increases smoothly because the vortex, still coherent, comes closer and closer to the probe driven by the remaining flow (this has been checked using simultaneously flow visualization and velocity measurements by the probe). The second part, with strong fluctuations, corresponds to the local velocity measured during and after the vortex has broken.

Data of the time recording $U(t_a)$ (where t_a denotes absolute time) are rescaled as follows: the velocity is first written as $U = u_m + u$, where u_m is the mean velocity, obtained averaging over the cycles and u is the fluctuation velocity. We then use $u_n(t) = u(t_a - t_n)$ where t_n denotes times at which the vortex breaks for each of the N cycles and we focus on $0 \le t \le T$ where $T \simeq 4.5$ s is the burst lifetime [Fig. 3(b)].

As in many experiments, our measurements are performed in the time domain while theoretical predictions are usually done in the spectral k domain. In the following, we work on a temporal windows $[t, t + \Delta t]$ and we note $E_{\Delta t}(k, t)$ the velocity power spectrum density (velocity PSD), averaged over the N cycles, for velocities $u_n(t \le t' \le t + \Delta t)$, recorded by the probe between t and $t + \Delta t$, and whose spatial scales are obtained using the local Taylor hypothesis $\delta r = \int_t^{t+\delta t} u_m(t')dt'$ ($\delta r \le \Delta r$ for $\delta t \le \Delta t$ and $0 \le t \le T$, $\Delta t \le T - t$). This hypothesis, first advocated in [11] and that can be found also detailed in [12–14] eliminates the bias on the velocity signal that the classical Taylor hypothesis (of frozen turbulence) introduces when large velocity fluctuation are considered (in our case, $\langle (U - \langle u_m \rangle)^2 \rangle^{1/2} / \langle u_m \rangle$ averaged on the turbulent part of the signal is of order 30%).

$E_{\Delta t}(k, t)$ has the significance of a time-averaged spectrum and it tends to an instantaneous energy spectrum $E(k, t)$ when Δt tends to zero.

Figure 4 shows the velocity PSDs averaged over the whole burst lifetime $\overline{E}(k) = E_T(k, 0)$ as a function of the distance d from the z axis. It can be seen that turbulent behavior with Kolmogorov $-5/3$ law is obtained near the place where the vortex explodes (here $d = 55$ mm) and progressively decays when going far away. The inertial range is $k_m \simeq 0.2\ \text{cm}^{-1} \ll k \ll k_M \simeq 2\ \text{cm}^{-1}$, in qualitative agreement with, for instance [15]: $k_m = 1/L\ \text{cm}^{-1}$ where L refers to the large scale motions responsible for

TABLE I. Characteristics of the vortex when it breaks. $u_\theta^{\max}$ denotes the maximum azimuthal velocity $u_\theta(r)$, reached for $r = r_0$ (r_0 the vortex core size), Γ denotes the circulation, and R the lateral extension of the vorticity (corresponding measurements can be found in [9]). Finally, a coarse estimation of the stretching $a \equiv \partial_x u_z$ is given (from [10]).

$u_\theta^{\max}$	τ_0	Γ	$\text{Re} = \Gamma/\nu$	R	a
$10\ \text{cm s}^{-1}$	0.6 cm	$40\ \text{cm}^2\ \text{s}^{-1}$	4 000	~ 3 cm	$1 - 10\ \text{s}^{-1}$

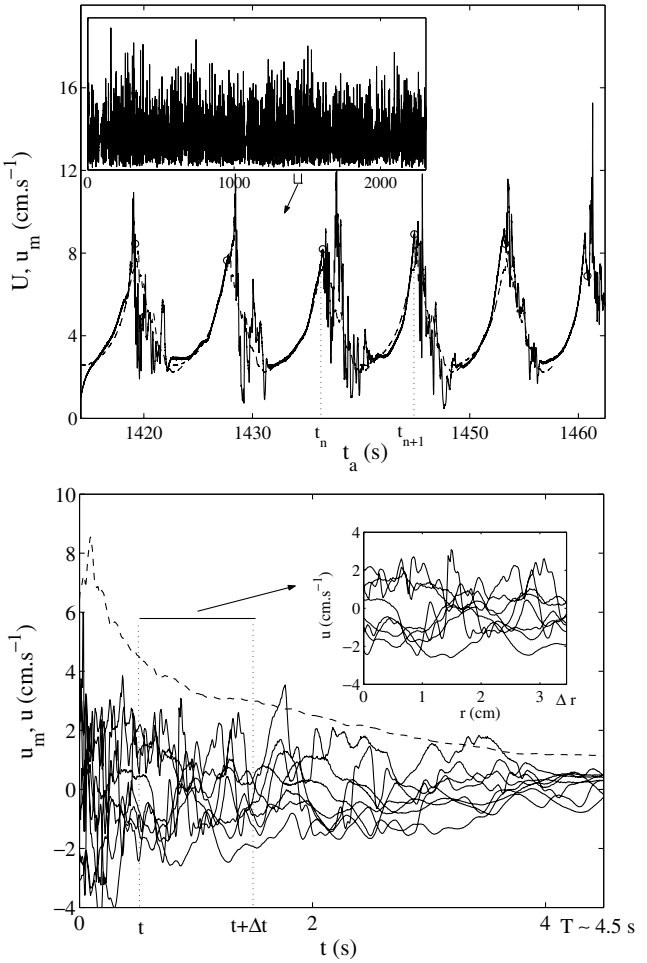

FIG. 3. (a) Close up over several vortex cycles of the full temporal recording (in subplot), $U(t_a)$ (−) and u_m (- -). (b) Rescaling for a few cycles $u_n(t) = u(t_a - t_n)$ (−); the inset shows the transformation $\delta t \to \delta r(t) = u_m(t)\delta t$ on a window $[t; t + \Delta t]$.

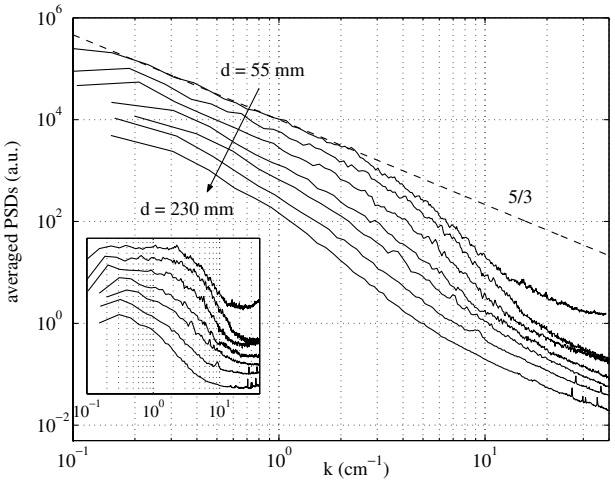

FIG. 4. Velocity PSD's averaged over the whole cycle $\overline{E}(k) = E_T(k, 0)$ for $d = 55, 65, 75, 85, 95\,135$, and 230 mm; the inset shows the compensated spectra $k^{5/3}\overline{E}(k)$.

the stretching ($L \simeq 12$ cm imposed by the distance between the two suction holes) and $k_M = \sqrt{a/\nu} \sim$ 10–30 cm^{-1}.

Figure 5 shows spectra $E_{\Delta t \simeq T/3}(k, t)$ calculated for $d =$ 55 mm and at $t = 0, T/3$, and $2T/3$, i.e., the three spectra averaged over each third of the burst life. Both Figs. 4 and 5 suggest that the turbulent vortex, i.e., leading to an inertial range with $k^{-5/3}$ behavior, has a lifetime shorter than the burst lifetime T: the whole turbulent spectrum is built in a time T_v of around $T/3 \simeq 1.5$ s in the region where the vortex breaks (the value of T_v will be defined more precisely from Fig. 6). Thereafter, the turbulence decays (in time and space).

Time T_v can be compared with the lifetime of a spiral limited by the process of viscous diffusion in the Lundgren model. In [7,16], the authors suggest that this lifetime behaves as $\tau_v = C(R^2/4\nu)\mathrm{Re}^{-2/3}$, where C is a constant (whose theoretical value is 15 and obtained in numerical computations equal to 10), R is the lateral extension of the vortex, Re the Reynolds number and where $\tau = (e^{at} - 1)/a$ is a stretched time variable. From Table I, we obtain 0.5 s $\leq t_v \leq$ 2.5 s, in qualitative agreement with the present value of T_v.

To better understand how the energy cascade builds up, we focus on the temporal evolution of the velocity PSD's during the lifetime of the vortex. Indeed, it is known that spiral structures give energy spectrum with a k^p range, the exponent p being different from $-5/3$ and depending on the flow field characteristics [7,15,17]. It is one remarkable property of the Lundgren's model that the time averaging produces the $k^{-5/3}$ law, independently of the details of the flow field structure. Similar behavior has been shown by [18] for vortices in two-dimensional flows (in that case, time averaging causes a k^{-2} spectrum to emerge).

Figure 6 shows the cumulative spectra $E_{\Delta t}(k, t = 0)$ between $t = 0$ and Δt for increasing values of Δt. Such velocity PSD tends to the instantaneous PSD $E(k, t = 0)$ for vanishing Δt and is equal to the PSD averaged over the whole burst lifetime $\overline{E}(k)$ for $\Delta t = T$, where a $k^{-5/3}$ behavior is expected (as seen on Fig. 4). The variation of the spectral slope p of $E_{\Delta t}(k, t = 0)$ when increasing Δt (in the inset of Fig. 6 [20]) is found to decrease from a value close to -1 for small times and it reaches the $-5/3$ value at T_v, thereafter it remains constant. This first representation allows us to conclude that the spectral slope indeed varies during the vortex lifetime. It also confirms that the whole spectrum is built in a time $T_v =$ 1.5 s (T_v can be accurately determined from Fig. 6 when p reaches $-5/3$).

To better describe the evolution of the spectra, one needs quasi-instantaneous spectra, which require one to

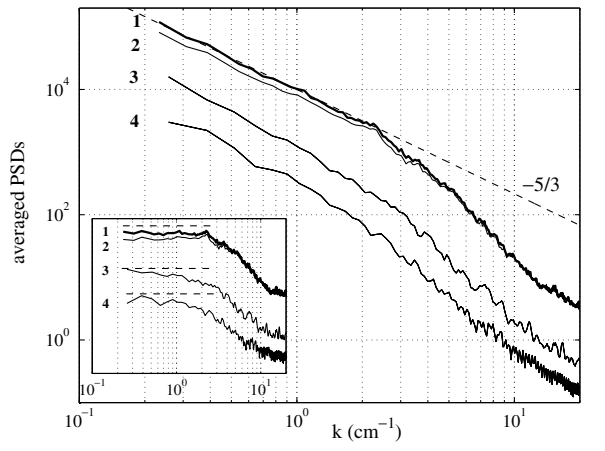

FIG. 5. Velocity PSD's averaged over a third cycle [**2** for $E_{\Delta t=1.5\ \mathrm{s}}(k, t = 0)$, **3** for $E_{\Delta t=1.5\ \mathrm{s}}(k, t = 1.5\ \mathrm{s})$, and **4** for $E_{\Delta t=1.5\ \mathrm{s}}(k, t = 3\ \mathrm{s})$] compared with the velocity PSD averaged over the whole cycle [**1** for $\overline{E}(k)$] at $d = 55$ mm; the inset shows the compensated spectra.

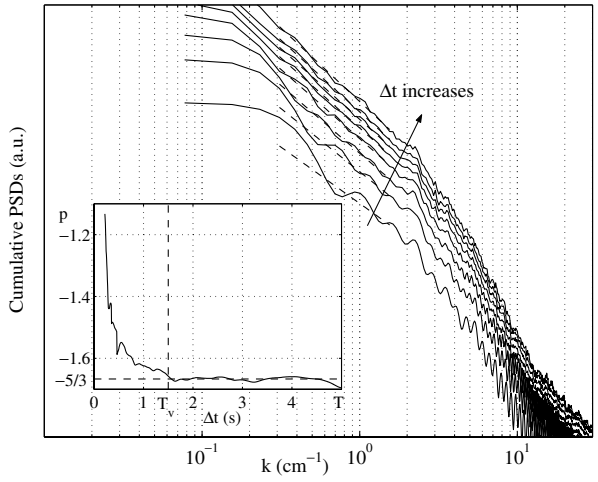

FIG. 6. Cumulative spectra $E_{\Delta t}(k, t = 0)$ for $\Delta t =$ 0.22, 0.35, 0.5, 0.75, 1, 1.25, 1.5, and 5 s (the fit in k^p is indicated in dotted lines); the inset shows p vs Δt.

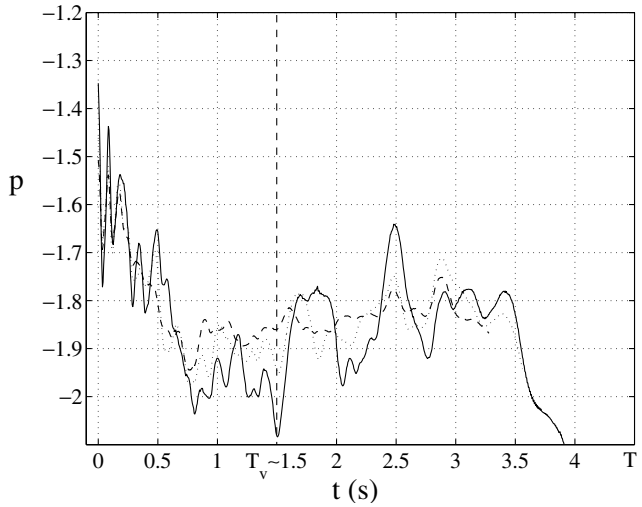

FIG. 7. k slope p of the quasi-instantaneous velocity PSDs vs time for $\Delta r = 1.6$ cm (−), $\Delta r = 2$ cm (..), and $\Delta r = 2.5$ cm (- -).

choose small values of Δt. As previously stated, the fit for p being obtained in the range $1/\Delta r \leq k \leq k_M$ is noisier for small Δr, i.e., small Δt. We impose, somewhat arbitrarily, that $\Delta r \geq R/2$. This allows us to keep at least 80% of the inertial range for the fit; we then adapt Δt at each t to maintain a fixed Δr. Figure 7 shows the results for $\Delta r = 1.5$, 2, and 2.5 cm. It is obvious that the slope of the instantaneous spectrum varies from a value close to -1 to a value close to -2 when time goes between 0 and T_v. Above $t = T_v$, the determination of the slope becomes more dependent on the value of Δr, suggesting that the velocity PSD's no longer follow a power law. It has to be noticed that this temporal evolution of the slope between 0 and T_v differs from numerical calculations performed on a Lundgren's single spiral vortex [7].

In conclusion, it has been shown that our vortex burst in a laminar-flow environment is responsible for the build up of the energy cascade. It is, to our best knowledge, the first time that a single isolated flow structure is identified to produce the part of the turbulent energy spectrum described by Kolmogorov's $k^{-5/3}$ law. Also, this structure seems to have some common feature with the theoretical one of Lundgren. In addition to qualitative agreements such as the inertial range and the vortex lifetime, an important result of the present Letter is the experimental evidence of the transition that instantaneous velocity PSD's experience during the vortex lifetime. These PSD's are shown to exhibit a range with a k^p behavior with $-2 \leq p \leq -1$, while time averaging results in a $k^{-5/3}$ behavior, as theoretically predicted by [15]. However, it has to be noticed that the evolution of p, from -1 to -2 with increasing time differs from numerical results of [7]. Study of the bidimensional dynamics, as performed in [19], could be helpful to explain this behavior.

Two other things seem worthwhile to do in the future, both related to the Lundgren's model. First, the study of the axisymmetric part of the Lundgren's vortex, referred to as the central core, is not reported in the present Letter. Preliminary results suggest that the velocity field of this central core could be related to the mean velocity u_m measured locally in the present experiment. For instance, $u_m(t)$ reasonably compares with the velocity $u_0(t) = \Gamma_0/2\pi(u_a t + r_i)$ that would be measured locally for an axisymmetric structure of circulation $\Gamma_0 \sim \Gamma$, advected by the velocity $u_a \simeq 0.5 u_{\text{mean}}$ (where u_{mean} is calculated with Q_1) and whose initial distance from the probe would be $r_i \simeq r_0$. Analyzing particle imaging velocimetry (PIV) images, notably by time averaging them, should provide further information for this hypothesis.

Second, the main characteristic of the Lundgren's vortex is the existence of spirals that should be identified in the physical domain. Again, the use of high resolution PIV should be helpful in this direction.

[1] T. S. Lundgren, Phys. Fluids **25**, 2193–2203 (1982).
[2] T. S. Lundgren and N. N. Mansour, J. Fluid Mech. **307**, 43–62 (1996).
[3] S. Childress, Geophys. Astrophys. Fluid Dyn. **29**, 29–64 (1984).
[4] A. Battacharjee, C. S. Ng, and X. Wang, Phys. Rev. E, **52**, 5110–5123 (1995).
[5] M. V. Melander and F. Hussain, Phys. Rev. E, **48**, 2669–2689 (1993).
[6] C. Simand, F. Chillá, and J.-F. Pinton, Europhys. Lett. **49**, 336–342 (2000).
[7] D. I. Pullin, J. D. Buntine, and P. G. Saffman, Phys. Fluids **6**, 3010–3027 (1994).
[8] P. Petitjeans *et al.*, Eur. J. Mech. B, Fluids, **17**, 549–560 (1998).
[9] S. Manneville *et al.*, Phys. Fluids **11**, 3380–3389 (1999).
[10] M. Rossi *et al.* (to be published).
[11] J.-F. Pinton and R. Labbe, J. Phys. II **4**, 1461–1468 (1994).
[12] R. Camussi, S. Ciliberto, and C. Baudet, Phys. Rev. E, **56**, 6181–6184 (1997).
[13] P. Marcq and A. Naert, Physica (Amsterdam) **124D**, 368–381 (1998).
[14] O. Chanal *et al.*, Eur. Phys. J. B **17**, 309–317 (2000).
[15] A. D. Gilbert, Phys. Fluids **5**, 2831–2834 (1993).
[16] D. I. Pullin and P. G. Saffman, Phys. Fluids **5**, 126–145 (1992).
[17] H. K. Moffat, in *Proceedings of the I.M.A. Conference*, edited by M. Farge, J. C. R. Hunt, and J. C. Vassilicos (Oxford University Press, London, 1993).
[18] A. D. Gilbert, J. Fluid Mech. **193**, 475–497 (1988).
[19] T. S. Lundgren, Phys. Fluids A **5**, 1472–1483 (1993).
[20] The fit $E_{\Delta t}(k, 0) \sim k^p$ is performed in the range $1/\Delta r \leq k \leq k_M$ when $\Delta r \leq k_m^{-1}$ and in the whole inertial range when $\Delta r > k_m^{-1}$. The determination of p is thus more and more significant when increasing Δt.